High Performance Bio-Inspired Analog Equalizer for DVB-S2 Non-Linear Communication Channel

M. Bauduin*, Q. Vinckier*, S. Massar†, F. Horlin*
mbauduin@ulb.ac.be
*Université Libre de Bruxelles (ULB) - OPERA department - CP 165/81, Avenue F.D. Roosevelt 50, 1050 Bruxelles, Belgium
†Université Libre de Bruxelles (ULB) - LIQ department - CP 224, Boulevard du Triomphe, 1050 Bruxelles, Belgium

***Abstract*—To ensure a high signal-to-noise power ratio at the terrestrial receiver, the power amplifier aboard the satellite often works close to its saturation point. Unfortunately, this operating point also adds non-linear distortions in the communication channel. The literature proposes several digital equalizers to compensate for this channel. But their complexity makes their digital implementation difficult in particular for high bandwidth communications. Analog equalizers are an interesting solution to reduce the equalizer complexity. Here we numerically demonstrate that a dedicated analog optoelectronic implementation based on the Echo State Network paradigm can reach state-of-the-art performance of digital equalizers, while reducing the required resolution of the analog-to-digital converters.**

***Index Terms*—Echo State Network, Non-linear Channel equalization, Satellite, Analog Equalizer**

I. Introduction

Satellite communications are specified by several communication standards such as the DVB-S2 (Digital Video Broadcasting - Satellite - Second Generation) [1]. In this scenario, the satellite works like a relay point between two terrestrial stations. The satellite receives a signal, amplifies it and retransmits it without digital signal processing.

Because of the limited power available aboard the satellite, the power amplifier must work close to the saturation point to ensure a high power output. This increases the amplifier efficiency but adds important non-linear distortions in the communication channel. In addition, inter-symbol interferences (ISI) appear if the channel bandwidth is increased. This is due to the limited bandwidth of the filters aboard the satellite. Together, these create a non-linear communication channel with memory. The literature proposes several digital algorithms to compensate for this channel at the receiving side. Many of them use a baseband Volterra structure for the equalization [2] [3].

Another family of digital equalizers is based on the Recurrent Neural Networks (RNNs) [4]. Because of the important number of parameters to train, they are complex to use in practice. Echo State Nework (ESN) are a form of RNN that have been introduced to reduce the training task complexity [5][6]. They have proven useful for tasks such as speech recognition or time-series prediction [7]. We showed in [8] that digital ESNs can reach similar performances as the Volterra equalizer with a similar or even lower algorithm complexity when the ESN parameters are optimized [9].

However, the complexity of these algorithms makes the digital implementation difficult because all the operations must be implemented with combinations of logical gates. It increases the latency and the power consumption of the receiver. On the other hand, with analog processing, these operations are directly provided by the behaviour of analog components. In that way, the transposition of the equalization from digital to analog domain can reduce the receiver complexity.

The equalization of a linear wireless communication channel with analog or mixed-signal solutions has been studied in [10] [11]. But, to the best of our knowledge, the compensation of a realistic non-linear communication channel with an analog equalizer has never been investigated.

Because of its structure, the ESN has the advantage that it can easily be implemented using analog circuits. Experimental implementations have been reported using optoelectronic [12] [13] and all-optical [14] [15] [16] circuits. In this paper, we propose an optoelectronic analog implementation dedicated to the non-linear satellite channel equalization. We show, with numerical simulations, that we can achieve similar performances as digital ESN and Volterra equalizers in term of Bit Error Rate (BER).

Furthermore, it is well known that the analog-to-digital converter (ADC) is a bottleneck for high bandwidth communications [10] [11] [17] because it is difficult to combine high sampling frequency with the important resolution required by digital equalizers. With our solution, the ADCs are situated at the output of the equalizer. They can be directly used as symbol detectors based on I and Q axes if no soft decoding is used on the symbols. This considerably reduces the number of required quantification bits. However, because of the constellation distortion introduced by the amplifier, the different received constellation points are no longer aligned. A simple pre-distortion of the transmitted constellation can modify the received one in order to improve the constellation points alignment on the I and Q axis. In that way, a considerable reduction in resolution of the ADC is possible.

We believe that the main results of our paper, namely that analog equalizers together with pre-distortion can reduce both the equalizer complexity and the resolution of the ADC, are very general and will apply to many other non-linear communication channels in addition to the specific DVB-S2

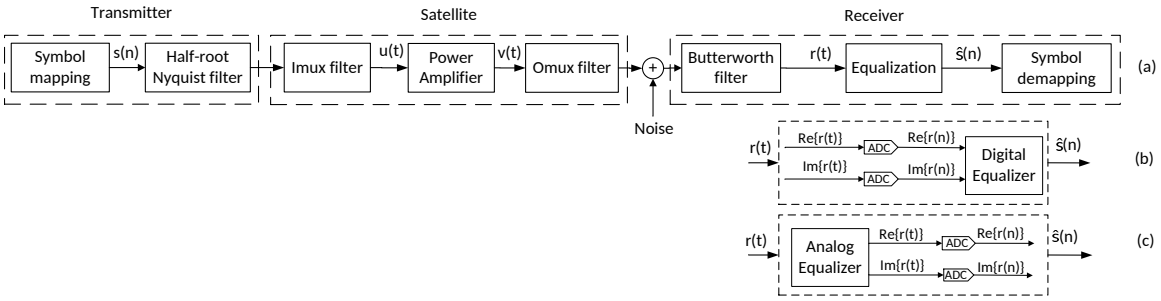

Fig. 1. Bloc diagram of a satellite communication channel, (a) Communication bloc, (b) Digital equalizer, (c) Analog equalizer.

channel studied here.

The outline of this paper is the following. The satellite communication channel is described in section 2. The ESN is introduced in section 3 with the equations of a digital implementation. Its optical implementation is described in section 4. The analog ESN is compared with its digital equivalent and a digital Volterra equalizer in term of BER in section 5.

II. System model

The baseband satellite communication channel, which is a non-linear channel with memory, is described on Fig. 1. The power amplifier aboard the satellite gives the non-linear behaviour of the channel. It is defined by its baseband model which gives the amplitude modulation $f_{\text{PA}}(.)$ and phase modulation $g_{\text{PA}}(.)$ characteristics. If the input is defined as $u(t)$, the output of the amplifier $v(t)$ is:

$$v(t) \quad = \quad f_{\text{PA}}(|u(t)|)e^{j(\angle u(t)+g_{\text{PA}}(|u(t)|))}. \tag{1}$$

The operating point is defined by the output back off (OBO) defined as

$$\text{OBO} = 20\log_{10}\frac{A_{\text{out}}}{A_{\text{sat}}}, \tag{2}$$

where A_{out} is the root mean square (rms) amplitude of the signal at the output of the power amplifier and A_{sat} is the saturation amplitude of the amplifier.

The memory of the channel comes from the Butterworh and the half-root Nyquist shaping filters at the ground station and the filters aboard the satellite. These latter can also be modelled by Butterworth low-pass filters.

The propagation channel is considered as memoryless because there is a line-of-sight communication between the satellite and the ground stations. The important directivity of the antennas reduces the reflections on obstacles.

On the transmitter side, the sequence of transmitted symbols is shaped with a half-root Nyquist filter and transmitted to the satellite. Then the signal is shaped with an imux filter, amplified with the power amplifier following eq. (1) and shaped with the omux filter. The received signal is also corrupted by an additive white Gaussian noise. At the receiving side, this signal is shaped with a Butterworth filter before the equalization to limit the noise power. The analog-to-digital conversion is done before (Fig. 1 (b)) or after (Fig. 1 (c)) the equalizer depending on the implementation (digital or analog). The sampling rate is equal to the symbol rate.

In a linear communication channel, the clusters of points which define the received constellation are centred on the transmitted one. But with a non-linear channel, the received constellation is affected by a compression due to the non-linear power amplifier. We can observe a displacement of the center of the cloud of points, called centroids [18].

III. Digital Echo State Network

The ESN is a framework which has been proposed to reduce the complexity of the learning task of RNNs. The algorithm is composed by N neurons $x_i(n)$ with $i = 0, ..., N-1$ connected to each other in a neural network. Here, we use a specific structure where each neuron $x_i(n)$ is only connected to the previous one at the previous time $x_{i-1}(n-1)$ in order to create a ring structure. It has been shown in [19] that this structure can offer the same performances as the random connections proposed initially. As we will see in next section, it simplifies the analog implementation.

The evolution of the neurons is defined by:

$$x_i(n) = f_{\text{NL}}(a_i(n)), \tag{3}$$

where $a_i(n)$ is the activation signal defined by:

$$\begin{cases} a_i(n) = \alpha x_{i-1}(n-1) + w_i^{\text{in}} r(n), & 0 < i \leq N-1 \quad (4) \\ a_i(n) = \alpha x_{N-1}(n-1) + w_i^{\text{in}} r(n), & i = 0 \quad (5) \end{cases}$$

where α is called the feedback gain and $r(n)$ is the received baseband signal. The input weights w_i^{in} are real random numbers with a uniform distribution limited to a specific range of values. The activation function $f_{\text{NL}}(.)$ creates the non-linear behaviour of the ESN. Here we propose the use of a new activation function compared to the ones used usually (e.g. a sine in [12], a tanh in [6] or a polynome in [8])

$$f_{\text{NL}}(a) = a.\sin(\frac{\pi}{2}|a|^2 + \gamma), \tag{6}$$

where γ is a bias optimized by simulations. We will see that this can easily be implemented with optoelectronic components. We also show that, as with the activation function used in [8] and [9], we achieve similar performances to the Volterra equalizer.

The output signal is defined by:

$$\widehat{s}(n) = \sum_{i=0}^{N-1} w_i^{\text{out}} x_i(n), \tag{7}$$

where w_i^{out} are the output weights. In classical RNNs, the weights w_i^{out}, w_i^{in} and the connections between the neurons are trained. But in the ESN paradigm, only the output weights are trained to implement a specific task. In that way, the number of connections that need to be optimized is strongly reduced which simplifies the training task without degrading the performances.

The ESN requires the echo state property (ESP) which specifies that the value of each neuron only depends on the past history of the input signal. In that way, the initial state of the ESN tends to be forgotten and will not affect the output signal $\widehat{s}(n)$. This property is respected if the activation function $f_{\text{NL}}(.)$ is Lipschitz continuous and the product of its Lipschitz constant with the spectral radius of the interconnection matrix is lower than 1 [20].

IV. Analog Implementation of the ESN

We propose an optoelectronic implementation of the ESN using coherent light. This implies that the information can be coded in both amplitude and phase of the light. A bloc diagram of this implementation is provided on Fig. 2. For the simplicity, we consider that no delay is introduced by the analog components, except the delay lines. This implementation is based on the recent work [21] and the optical implementations [16] [22] adapted to give good performance for the present task.

In a first step, we need to recover the amplitude $|r(t)|$ of the received baseband signal $r(t)$ and a signal proportional to its phase $\angle r(t)$. These electrical signals are maintained constant during a symbol duration T with a sample-and-hold circuit.

Then the signal $|r(t)|$ is multiplied with the input mask $w^{\text{in}}(t)$ which is a stepwise periodic signal of N steps with period T. Each value is maintained during $\theta = \frac{T}{N}$ seconds. The values of the input mask w_i^{in} are coded in $w^{\text{in}}(t)$ for $nT + i\theta < t \leq nT + (i+1)\theta$.

A continuous-wave laser beam is modulated by a voltage driven intensity modulator (Lithium Niobate Mach-Zehnder interferometer M-Z), to code $w^{\text{in}}(t)|r(t)|$, and a phase modulator, to code $\angle r(t)$ (part (1) of Fig. 2). The linear transfer function of the phase modulator and the sinusoidal transfer function of the M-Z lead to an input signal at the entrance of the first optical loop defined by:

$$f_{\text{in}}(w^{\text{in}}(t), r(t)) = \sin(\frac{\pi}{2} w^{\text{in}}(t)|r(t)|) e^{j\angle r(t)}. \tag{8}$$

All the neurons are temporally multiplexed in the first loop (part (2) of Fig.2). So, in one specific position, the neuron $x_i(n)$ is coded in the analog signal $x(t)$ when $nT + i\theta < t \leq nT + (i+1)\theta$.

The activation function $f_{\text{NL}}(.)$ which creates the signal $x(t)$ from the activation signal $a(t)$ is implemented with a photodiode and a second M-Z in the first optical loop. The photodiode produces an electrical signal proportional to the square amplitude of the optical signal at its input. The bias γ is created with a constant voltage applied on the M-Z.

This loop has a round trip time of duration $T' = \theta(N+1)$ [12]. In that way, the evolution of $a(t)$ defined on the middle of an interval of duration θ is:

$$\begin{aligned} a(nT + (i+0.5)\theta) &= \alpha x(nT + (i+0.5)\theta - T') \\ &\quad + f_{\text{in}}(w^{\text{in}}(nT + (i+0.5)\theta), r(nT + (i+0.5)\theta)), \end{aligned} \tag{9}$$

where

$$x(t) = a(t)\sin(\frac{\pi}{2}|a(t)|^2 + \gamma). \tag{10}$$

As $r(t)$ is constant during T seconds and because the input mask $w^{\text{in}}(t)$ is a periodic signal, it is equivalent to:

$$\begin{aligned} a(nT + (i+0.5)\theta) &= \alpha x((n-1)T + (i-0.5)\theta) \\ &\quad + f_{\text{in}}(w^{\text{in}}((i+0.5)\theta), r(nT)). \end{aligned} \tag{11}$$

So it is equivalent to the digital ESN described by eq. (4) and (5) where each neuron $x_i(n)$ is connected to the previous one $x_{i-1}(n-1)$, except for the neuron $x_0(n)$ which is now connected to $x_{N-1}(n-2)$. The required feedback gain α is fixed by the couplers coefficients.

The neurons $x(t)$ at the output of the loop are multiplied with the output mask $w^{\text{out}}(t)$ using a third M-Z and a second phase modulator to produce the signal $y(t)$ (part (3) of Fig. 2). This produces a signal defined by:

$$y(t) = x(t) w^{\text{out}}(t). \tag{12}$$

The output mask is a stepwise periodic signal of N steps. The values of the output mask w_i^{out} are coded in $w^{\text{out}}(t)$ when $nT + i\theta < t \leq nT + (i+1)\theta$. An experimental implementation of an analog output is provided in [22].

The summation of the weighted neuron states $y(t)$ is done in the second optical loop which acts as an optical integrator (part (4) of Fig. 2) [21]. Its round trip duration is equal to θ.

The output mask must take into account the exponential decay of the second loop impulse response $h(t)$:

$$h(t) \propto e^{-\alpha_{\text{OI}} t}, \tag{13}$$

where α_{OI} is the feedback gain of the optical integrator. It is fixed by the two optical couplers of the loop.

The output of the optical integrator is given by:

$$\widehat{s}(t) = \int_0^{\infty} y(t-\tau) h(\tau) d\tau. \tag{14}$$

The signal $\widehat{s}(t)$ is sampled with a sampling period T. At time nT, we have:

$$\widehat{s}(nT) = \sum_{m=0}^{\infty} y(nT - m\theta) h(m\theta). \tag{15}$$

This equation is equivalent to:

$$\widehat{s}(nT) = \sum_{i=0}^{N-1} w^{\text{out}}(T - i\theta) \tilde{x}_i(nT), \tag{16}$$

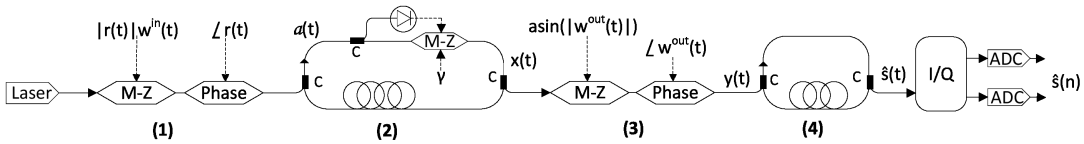

Fig. 2. Structure of the optical implementation of the ESN where the dashed lined are electrical signals and the continuous lines are optical signals. The input mask is implemented on part (1). The part (2) concerns the neural network itself. Part (3) and (4) concern the output mask. Part (2) and (4) are optical loop with delay line. The input and output of each loop is defined with optical couplers C. The neurons will be processed sequentially. The real and imaginary part of the equalized signal $\widehat{s}(t)$ can be recovered with a 90° optical hybrid.

where

$$\tilde{x}_i(nT) = \sum_{j=0}^{\infty} x(nT - jT - i\theta)h(jT + i\theta). \qquad (17)$$

This expression is used to evaluate the weights $w^{\text{out}}(t)$ which pre-compensate $h(t)$. Let us note that the exponential decay of $h(t)$ must be slow enough so that all the neurons contribute significantly to eq. (16).

Note that the optical loops are very sensitive to any kind of perturbations (e.g. temperature variation, vibration) which can modify their length and introduce phase noise. For experimental implementations, a regulation process is thus required. For example, one can adjust the length of the optical loops with a piezoelectric stretcher [16].

In experimental implementations, the input and output masks are generated with Arbitrary Waveform Generators [12] [14] [16]. This limits the ESN speed because of the high bandwidth required by these masks. An analog implementation of these operations should be investigated to avoid this constraint and fully exploit the capacities of analog ESNs.

V. Numerical results

We consider a 16-QAM modulation. The imux and omux filters have a 36 MHz bandwidth. The symbol rate is 30 MHz. The shaping filter on the terrestrial receiver is an order 3 Butterworth filter with a cut-off frequency equal to the symbol rate. The roll-off of the half-root Nyquist filer is fixed at 0.25. The operating point of the power amplifier is defined by a -2 dB OBO. For the channel, we use the model proposed in [1]. The functions $f_{\text{PA}}(.)$ and $g_{\text{PA}}(.)$ are described with a Ghorbani model [23]:

$$f_{\text{PA}}(u(t)) = \frac{q_1|u(t)|^{q_2}}{1 + q_3|u(t)|^{q_2}} + q_4|u(t)|, \qquad (18)$$

$$g_{\text{PA}}(u(t)) = \frac{q_5|u(t)|^{q_6}}{1 + q_7|u(t)|^{q_6}}, \qquad (19)$$

where the following values are used: $q_1 = 6$, $q_2 = 1.3$, $q_3 = 3.3$, $q_4 = -0.4$, $q_5 = 1.8$, $q_6 = 1.8$, $q_7 = 1.4$.

A simulation of the analog ESN described in section 4 is compared to two digital equalizers. Namely, the Volerra equalizer widely used in the state-of-the-art and the ESN described in section 3. The latter is similar to the digital solutions proposed in [8] [9].

The ESN and the Volterra filter are trained to recover a constellation defined on the centroids of the received signal as described in [8]. In that way, the equalizers will only compensate for the interferences and not the compression of the constellation. We consider that the channel is fixed and the coefficients of the equalizers are known in advance.

The digital and analog ESNs have a feedback gain α of 0.35 and a bias γ of 0.5. Their input mask is composed of random values with a uniform distribution between -0.2 and 0.2 for an input signal $r(t)$ with a rms amplitude of 1. The integration loop of the analog ESN has a feedback gain α_{OI} of 0.95. These values have been determined on the basis of extensive simulations. Both ESNs are composed of 85 neurons. The Volterra equalizer has a linear memory of size 10 and an order 3 memory of size 5. It is therefore also composed by 85 coefficients [2]. We can see on Fig. 3 that the three solutions offer similar performances.

In order to use low resolution ADCs at the output of the analog equalizer, a pre-distortion of the transmitted constellation is required. This improves considerably the alignment of the centroids on the I and Q axis (see Fig. 4). As a consequence, we can use a 2 bits ADC per axis at the cost of a slight BER degradation (see Fig. 5). The slight degradation is due to the fact that the alignment of the constellation points cannot be made perfect at this high OBO.

With digital implementations, the ADCs are situated before the equalizer. Fig. 5 shows that in this case the BER degradation is more important with low resolution ADCs.

VI. Conclusion

We have shown by simulations that an analog implementation of the ESN can be as efficient as a digital one. We have similar performances as the digital Volterra equalizer used in the state-of-the-art with identical number of adjustable coefficients. In addition, we found that the analog equalizer is an interesting approach to reduce the number of quantization bits of the ADCs. In parallel, several experimental implementations of the ESN have been reported in the literature. This shows the viability of this approach to compensate a non-linear communication channel.

References

[1] Digital video broadcasting (dvb) second generation: Framing structure, channel coding and modulation systems for broadcasting, interactive

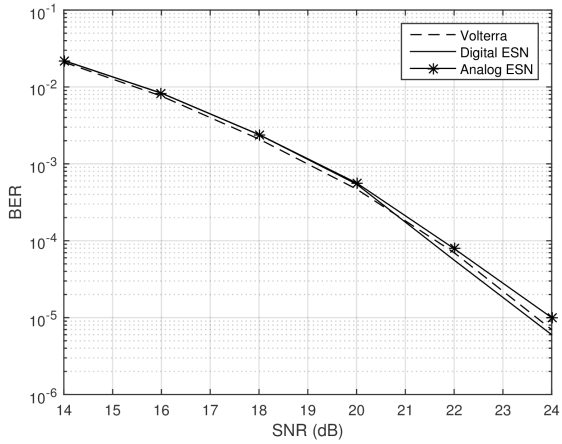

Fig. 3. Performance comparison between digital equalizers and analog ESN. Each equalizer has 85 adjustable coefficients.

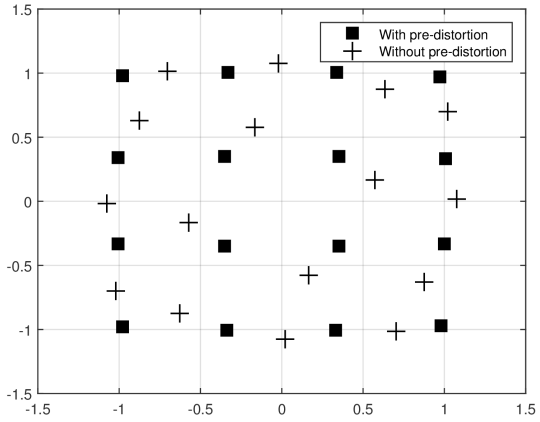

Fig. 4. Centroids of a received constellation with and without pre-distortion on the transmitter side

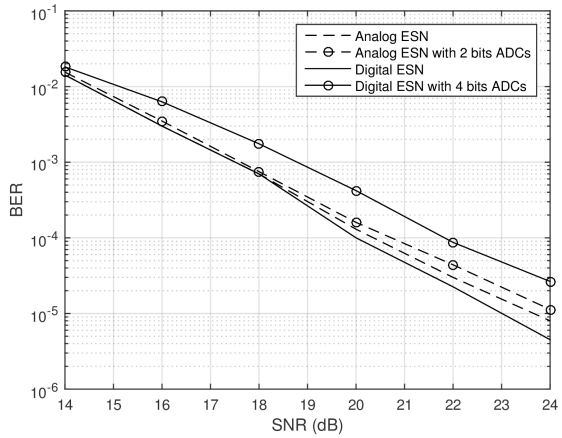

Fig. 5. Performance comparison between digital and analog ESN with a pre-distorted constellation when the number of quantization bits of the ADC is reduced.

services, news gathering and other broad band satellite application, etsi en 302 307 version 1.2.1. ETSI, April 2009.

[2] S. Benedetto. Principles of Digital Transmission: With Wireless Applications. Kluwer, 1999.

[3] A. Gutierrez and W. E. Ryan. Performance of adaptative volterra equalizers on nonlinear satellite channels. IEEE International Conference on Communication, Vol.1, p.488-492, June 1995.

[4] G. Kechriotis, E. Zervas, and E.S. Manolakos. Using recurrent neural networks for adaptive communication channel equalization. IEEE Transactions on Neural Networks, vol.5, issue 2, p.267-278, March 1994.

[5] H. Jaeger. The "echo state" approach to analysing and training recurrent neural networks. Fraunhofer Institute for Autonomous Intelligent Systems, Technical report 148, 2001.

[6] M. Lukosevicius and H. Jaeger. Reservoir computing approaches to reccurent neural network training. Computer Science Review 3, Elsevier, pp 127-149, 2009.

[7] M. Lukosevicius, H. Jaeger, and B. Schrauwen. Reservoir computing trends. KI - Künstliche Intelligenz, pp. 1-7, May 2012.

[8] M. Bauduin, A. Smerieri, S. Massar, and F. Horlin. Equalization of the non-linear satellite communication channel with an echo state network. IEEE 81st Vehicular Technology Conference, May 2015.

[9] M. Bauduin, S. Massar, and F. Horlin. Non-linear satellite channel equalization based on a low complexity echo state network. 50th Annual Conference on Information Sciences and Systems, 2016, Accepted.

[10] D. A. Sobel and R. W. Brodersen. A 1 gb/s mixed-signal baseband analog front-end for a 60 ghz wireless receiver. IEEE Journal of Solid-State Circuits, vol. 4, no. 4, p. 1281-1289, April 2009.

[11] X. Feng, G. He, and J. Ma. A new approach to reduce the resolution requirement of the adc for high data rate wireless receivers. IEEE 10th International Conference on Signal Processing, p. 1565 - 1568, October 2010.

[12] Y. Paquot, F. Duport, A. Smerieri, J. Dambre, B. Schrauwen, M. Haelterman, and S. Massar. Optoelectronic reservoir computing. Scientific Reports 2, 287, February 2012.

[13] L. Larger and al. Photonic information processing beyond turing: an optoelectronic implementation of reservoir computing. Optics Express 20, pp. 3241-3249, 2012.

[14] F. Duport, B. Schneider, A. Smerieri, M. Haelterman, and S. Massar. All-optical reservoir computing. Optics Express 20, pp. 22783-22795, 2012.

[15] D. Brunner, M. C. Soriano, C. R. Mirasso, and I. Fischer. Parallel photonic information processing at gigabyte per second data rates using transient state. Nature Communications 4, 1364, 2013.

[16] Q. Vinckier, F. Duport, A. Smerieri, K. Vandoorne, P. Bienstman, M. Haelterman, and S. Massar. High-performance photonic reservoir computer based on a coherently driven passive cavity. Optica, vol. 2, no. 5, p. 438-446, May 2015.

[17] K. Hassan, T. S. Rappaport, and J. G. Andrews. Analog equalization for low power 60 ghz receivers in realistic multipath channels. IEEE Global Telecommunications Conference (GLOBECOM 2010), pp. 1-5, December 2010.

[18] R. De Gaudenzi and M. Luise. Analysis and design of an all-digital demodulator for trellis coded 16-QAM transmission over a nonlinear satellite channel. IEEE Transaction on Communication, Vol. 43, No. 2, pp 659-668, February 1995.

[19] P. Tino A. Rodan. Minimum complexity echo state network. IEEE Transactions On Neural Networks, Vol 22, Issue 1, pp 131-144, January 2011.

[20] R. Labahn T. Strauss, W. Wustlich. Design strategies for weight matrices of echo state networks. Neural Computation, MIT Press, vol. 24, issue 12, pp. 3246-3276, January 2012.

[21] Q. Vinckier, M. Haelterman, and S. Massar. Information processing using an autonomous all-photonic reservoir computer based on coherently driven passive cavities. Frontiers in Optics. Optical Society of America, October 2015.

[22] F. Duport, A. Smerieri, A. Akrout, M. Haelterman, and S. Massar. Analog photonic reservoir computer. Scientific Reports, 6, 22381, 2016.

[23] A. Ghorbani and M. Sheikhan. The effect of solid state power amplifiers (sspas) nonlinearities on mpsk and m-qam signal transmission. Sixth International Conference on Digital Processing of Signals in Communications, 193 - 197, September 1991.